Journal of Glaciology, Vol. 25, No. 93, 1980

FIRN DENSIFICATION: AN EMPIRICAL MODEL

By MICHAEL M. HERRON *and* CHESTER C. LANGWAY, JR

(Ice Core Laboratory, Department of Geological Sciences, State University of New York at Buffalo, 4240 Ridge Lea Road, Amherst, New York 14226, U.S.A.)

ABSTRACT. An empirical model of firn densification from the surface to the zone of pore close-off has been constructed. Fundamental rate equations have been derived for the first two stages of densification. In the first stage, for densities less than 0.55 Mg m^{-3}, the densification rate is proportional to the mean annual accumulation times the term $(\rho_i - \rho)$, where ρ is the density of the snow and ρ_i is the density of pure ice. The densification rate in the second stage, where 0.55 Mg $m^{-3} < \rho < 0.8$ Mg m^{-3}, is proportional to the square root of the accumulation rate and to $(\rho_i - \rho)$. Depth–density and depth–age calculations from this model are compared with observation. Model accumulation rates are within about 20% of values obtained by other techniques. It is suggested that depth intervals of constant density in some Antarctic cores may represent a synchronous event in the 1880's when ten times the normal accumulation fell within a year or two.

RÉSUMÉ. *Densification du névé: un modèle empirique.* On a construit un modèle empirique de la densification du névé depuis la surface jusqu'à la zone de fermeture des pores. Dans le premier stade, pour des densités inférieures à 0,55 Mg/m^{-3}, la vitesse de densification est proportionnelle au produit de l'accumulation moyenne annuelle par le terme $(\rho_i - \rho)$, où ρ est la densité de la neige et ρ_i la densité de la glace pure. La vitesse de densification dans le second stade, lorsque 0,55 Mg $m^{-3} < \rho <$ 0,8 Mg m^{-3}, est proportionnelle au produit de la racine carrée du taux d'accumulation par $(\rho_i - \rho)$. Des valeurs de la densité selon la profondeur, et de la densité selon l'âge sont calculées à partir de ce modèle et comparées avec l'observation. Les vitesses d'accumulation tirées du modèle restent à 20% près voisines des valeurs obtenues par d'autres techniques. On suggère que des tronçons de densité constante trouvés dans des carottes prélevées en Antarctique peuvent représenter un épisode vers les années 1880 où il est tombé dix fois plus de neige que la normale en un ou deux ans.

ZUSAMMENFASSUNG. *Firnverdichtung: ein empirisches Modell.* Für die Verdichtung des Firns von der Oberfläche bis zur Zone des Porenschlusses wurde ein empirisches Modell entwickelt. Für die beiden ersten Stufen der Verdichtung werden fundamentale Geschwindigkeitsgleichungen hergeleitet. In der ersten Stufe, für Dichten von weniger als 0,55 Mg m^{-3}, ist die Verdichtungsrate proportional dem Produkt aus der mittleren jährlichen Akkumulation und dem Ausdruck $(\rho_i - \rho)$, wobei ρ die Dichte des Schnees und ρ_i die des reinen Eises ist. Die Verdichtungsrate in der zweiten Stufe, wo 0,55 Mg $m^{-3} < \rho <$ 0,8 Mg m^{-3} gilt, ist proportional zur Quadratwurzel aus der Akkumulationsrate, multipliziert mit $(\rho_i - \rho)$. Berechnungen der Dichte und des Alters mit der Tiefe aus diesem Modell werden mit Beobachtungen verglichen. Die Modell-Akkumulationsraten stimmen auf etwa 20% mit Werten überein, die mit anderen Methoden gewonnen wurden. Die Annahme erscheint gerechtfertigt, dass Intervalle konstanter Dichte in einigen antarktischen Eiskernen aus einem gleichzeitigen Ereignis in den 80er Jahren des letzten Jahrhunderts stammen, bei dem innerhalb eines Jahres oder zweier die Akkumulation zehnmal grösser war als sonst.

INTRODUCTION

The transformation of snow into glacial ice is one of the most fundamental processes in glaciology. A number of theories regarding the dry densification of snow and firn have been proposed (Robin, 1958; Benson, 1959, 1962; Bader, 1960, 1962; Costes, 1963; Anderson and Benson, 1963; Kojima, 1964; Hobbs, 1968; Gow, 1975; Johnsen, 1977) and yet the relative importance of possible component processes such as settling, sublimation, recrystallization, volume diffusion, surface diffusion, and other deformation processes has not been firmly established. Consequently, it has not been possible to develop a theoretically based model which accurately predicts the depth–density profile from a given site without first obtaining seismic compressional-wave velocity data (Kohnen, 1972) or laboratory measurements on deep firn samples from that location.

Three stages of densification have been identified. The densification rate in the first stage, from initial snow density to the "critical density" of about 0.55 Mg m^{-3} (Benson, 1962; Anderson and Benson, 1963), is usually the most rapid. The dominant mechanism is considered to be grain settling and packing. Densities increase more slowly with depth in the second stage until the intercommunicating air passages become closed off to form individual bubbles at densities of 0.82–0.84 Mg m^{-3}. The mechanisms involved are not well understood. In the third stage, below the pore close-off zone, air can no longer be excluded and further densification takes place by compression of the bubbles (Langway, 1958; Bader, 1965). It is

generally recognized that the form of depth–density profiles depends on the snow accumulation rate and temperature. Higher temperatures and lesser accumulation rates result in the greatest change of density with depth.

The purpose of the present work is to derive an empirical, but widely applicable, model of the first and second stages of polar snow densification with the aid of depth–density data from recently recovered Greenland and Antarctic ice cores. Such a model would be of use to glaciologists and ice drilling engineers if the depth–density, depth–load, and depth–age profiles and the approximate pore close-off depth could be predicted from the commonly measured variable of mean annual temperature and mean annual accumulation rate. It is hoped that the model and the density data may also aid others in developing a better physical understanding of the densification process.

The model

Following Sorge's Law (Bader, 1954), the relation between snow density ρ and the depth h below the snow surface is assumed invariant with time under conditions of constant snow accumulation and temperature. Thinning of annual layers by plastic flow (Nye, 1963), a relatively minor effect in the upper layers of most inland ice sheets, is ignored.

Depth–density information was obtained from 17 sites in Greenland and Antarctica where mean annual temperatures range from $-57°C$ to $-15°C$ and annual accumulation rates range from 0.022–0.5 m water year^{-1} (Table I). The drilling techniques and reliability of the data are found in some of the original references. Temperatures used in this model are those at the 10 m depth and measurement accuracy is generally ± 0.1 deg or better. All densities were determined from measurements of the mass and dimensions of sections of core. Because of firn permeability, the highly accurate method of hydrostatic weighing (Butkovich, 1953) is impractical. Measurement accuracy is frequently ± 0.001 Mg m^{-3} although individual data points may exhibit more scatter due to seasonal variations in density or the presence of melt features. There is often a large uncertainty in the annual accumulation values due to imprecision in the identification of annual layers, short-range geographical and temporal variations, and the relatively short time period for which data are available.

The model is based on Robin's (1958) suggestions that in the densification of firn the proportional change in air space is linearly related to the change in stress due to the weight of overlying snow. Schytt (1958) expressed this as:

$$\frac{\mathrm{d}\rho}{\rho_i - \rho} = \text{constant } \rho \, \mathrm{d}h, \tag{1}$$

where ρ_i is the density of ice (0.917 Mg m^{-3}), which implies a linear relationship between $\ln [\rho/(\rho_i - \rho)]$ and depth. Schytt found such a relationship in the Maudheim core data.

To explore the widespread applicability of Equation (1) and the nature of the "constant" therein, depth–density information from the other available sites was plotted as $\ln [\rho/(\rho_i - \rho)]$ versus depth (Appendix). Temperature and pressure corrections for the density of pure ice make insignificant changes in $\ln [\rho/(\rho_i - \rho)]$ over the density range involved and a value of $\rho_i = 0.917$ Mg m^{-3} was used throughout. The plots generally consisted of two linear segments, one for $\rho < 0.55$ Mg m^{-3}, and a steeper slope for 0.55 Mg m^{-3} $< \rho <$ 0.8 Mg m^{-3}, corresponding to the first and second stages of densification. Although pore close-off occurs at $\rho = 0.82 - 0.84$ Mg m^{-3}, many of the plots were linear only through $\rho \doteq 0.8$ Mg m^{-3} with a much greater densification rate at the zone of pore close off. The pronounced influence of ice layers in cores from warmer sites such as Maudheim (Schytt, 1958), Roi Baudouin (Tongiorgi and others, 1962), and Dye 2 is evidenced by the scatter in the profiles. Only the $\rho < 0.55$ Mg m^{-3} portion of the Roi Baudouin site was used in the derivation of the model.

TABLE I. GLACIOLOGICAL DATA FOR GREENLAND AND ANTARCTIC ICE CORES

Site	Location		A	T	References for ρ, T, A data
	Latitude	Longitude	m water year^{-1}	°C	
			Greenland		
North Central	74° 37′ N.	39° 36′ W.	0.11	−31.7	This work
Crête	71° 07′ N.	37° 19′ W.	0.265	−30	This work; personal communication from B. L. Hansen; Hammer and others (1978); Reeh and others (1978)
Site 2	76° 59′ N.	56° 04′ W.	0.4	−23.3	Langway (1970)
Milcent	70° 18′ N.	44° 19′ W.	0.50	−22	This work; personal communication from B. L. Hansen; Hammer and others (1978); Reeh and others (1978)
South Dome	63° 33′ N.	44° 36′ W.	0.50	−21.5	This work; personal communication from W. Dansgaard
Dye 3	65° 11′ N.	43° 50′ W.	0.50	−19.6	This work; personal communication from B. L. Hansen; Hammer and others (1978); Reeh and others (1978)
Dye 2	66° 29′ N.	46° 20′ W.	0.5	−16.7	This work
			Antarctica		
Vostok	78° 28′ S.	106° 48′ E.	0.022	−57	Barkov (1973); Barkov and others (1974)
South Pole	90° S.		0.07	−51	This work; Gow (1968)
Old Byrd Station	79° 59′ S.	120° 01′ W.	0.16	−28	Gow (1968)
Roosevelt Island Dome	79° 22′ S.	161° 40′ W.	0.2	−22.7	This work; personal communication from H. B. Clausen and W. Dansgaard
Wilkes S-2	66° 29′ S.	112° 17′ E.	0.133	−19.4	Hollin and Cameron (1960)
			Antarctic ice shelves		
J-9	82° 22′ S.	168° 40′ W.	0.09	−27.9	This work; personal communication from J. Rand; Clausen and Dansgaard (1977)
C-7-3	78° 20′ S.	179° 51′ E.	0.11	−25.6	This work
Little America V	78° 10′ S.	162° 13′ W.	0.22	−24	Gow (1968)
Maudheim	71° 03′ S.	10° 56′ W.	0.37	−17	Schytt (1958)
Roi Baudouin	70° 26′ S.	24° 19′ E.	0.38	−15	Tongiorgi and others (1962)

The slopes of the linear segments, fitted by a least-squares method or, in some cases, by eye, may be represented as

$$C = \frac{\mathrm{d} \ln [\rho/(\rho_\mathrm{i}-\rho)]}{\mathrm{d}h} \qquad \text{for } \rho < 0.55 \text{ Mg m}^{-3}, \tag{2a}$$

and

$$C' = \frac{\mathrm{d} \ln [\rho/(\rho_\mathrm{i}-\rho)]}{\mathrm{d}h} \qquad \text{for } 0.55 \text{ Mg m}^{-3} < \rho < 0.8 \text{ Mg m}^{-3}, \tag{2b}$$

where C and C' are constants for each site. To solve for the densification rate, $\mathrm{d}\rho/\mathrm{d}t$, Equations (2a) and (2b) are rearranged with the substitution $\mathrm{d}h/\mathrm{d}t = A/\rho$, where A is the accumulation rate in water-equivalent units:

$$\mathrm{d}\rho/\mathrm{d}t = \frac{CA}{\rho_\mathrm{i}}(\rho_\mathrm{i}-\rho), \qquad \rho < 0.55 \text{ Mg m}^{-3}, \tag{3a}$$

https://doi.org/10.3189/S0022143000015239 Published online by Cambridge University Press

and

$$\mathrm{d}\rho/\mathrm{d}t = \frac{C'A}{\rho_i}(\rho_i - \rho), \qquad 0.55\ \mathrm{Mg\ m^{-3}} < \rho < 0.8\ \mathrm{Mg\ m^{-3}}. \tag{3b}$$

Equations (3a) and (3b) are equivalent to Equation (1). However, since the accumulation rate and temperature are fairly constant at each site, the functional dependencies of C and C' on T and A are unknown. We have assumed that the temperature and accumulation-rate dependencies may be separated and that the rate equations are of the form

$$\mathrm{d}\rho/\mathrm{d}t = k_0 A^a(\rho_i - \rho), \qquad \rho < 0.55\ \mathrm{Mg\ m^{-3}}, \tag{4a}$$

and

$$\mathrm{d}\rho/\mathrm{d}t = k_1 A^b(\rho_i - \rho), \qquad 0.55\ \mathrm{Mg\ m^{-3}} < \rho < 0.8\ \mathrm{Mg\ m^{-3}}, \tag{4b}$$

where k_0 and k_1 are Arrhenius-type rate constants dependent only on temperature and a and b are constants dependent on the densification mechanisms. Values of a and b may be determined by comparing slopes for each stage of densification at sites of nearly equivalent temperature and different accumulation rates using

$$a = \frac{\ln (C_1/C_2)}{\ln (A_1/A_2)} + 1, \tag{5}$$

and similarly for b by substituting C' for C into Equation (5). Values determined in this manner (Table II) are $a = 1.1 \pm 0.2$ and $b = 0.5 \pm 0.2$. Taking the values of a and b as 1 and 0.5, respectively, this model agrees with Robin's (1958) description of the densification process for the first stage, but not for the second.

TABLE II. VALUES OF THE CONSTANTS a AND b DERIVED FROM ACCUMULATION RATES AND SLOPES DERIVED FROM GRAPHS OF DEPTH AGAINST $\ln [\rho/(\rho_i - \rho)]$ FOR PAIRS OF SITES

Site pair	a	b
Site 2–RID	0.8	0.3
Site 2–Milcent	1.2	ID
Site 2–LAS	1.0	0.6
Site 2–C-7-3	1.1	0.6
C-7-3–LAS	1.2	0.7
C-7-3–Old Byrd	1.4	0.4
Old Byrd–J-9	1.4	0.3
RID–Milcent	0.9	0.5
RID–South Dome	ID*	0.3
LAS–Milcent	1.1	ID
Wilkes S2–Dye 3	ID	0.5
Crête–North Central	ID	0.6
Average and standard deviation	1.1 ± 0.2	0.5 ± 0.2

* ID = Insufficient data.

Values of the rate constants were deduced for each site and the general equations of k_0 and k_1 were determined from Arrhenius plots of $\ln k$ against $1/T$ (Fig. 1).

$$k_0 = 11 \exp\left[-\frac{10\,160}{RT}\right], \tag{6a}$$

and

$$k_1 = 575 \exp\left[-\frac{21\,400}{RT}\right], \tag{6b}$$

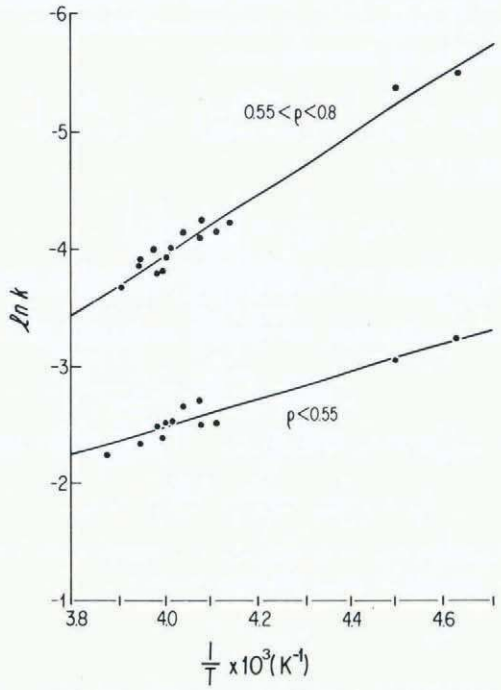

Fig. 1. Arrhenius plots for k_0 (lower line) and k_1 (upper line).

where R is the gas constant (8.314 J K^{-1} mol^{-1}) and T is the temperature in kelvins. The correlation coefficients between the logarithms of the rate constants and reciprocal temperature are 0.959 for k_0 and 0.987 for k_1. S. J. Johnsen has kindly pointed out that Equation (4b) may be rewritten in terms of load σ as:

$$\frac{d\rho}{dt} = k_1^2 \frac{(\sigma_\rho - \sigma_{0.55})(\rho_i - \rho)}{\ln [(\rho_i - 0.55)/(\rho_i - \rho)]}, \tag{4c}$$

for which the apparent activation energy is 42.6 kJ/mol. This value is more in line with values for known physical processes in ice. However, the utility of Equation (4b) lies in the ease of calculation of density profiles or accumulation rates when one of these and the mean annual temperature are available.

Depth–density and depth–age calculations

Given T, A, and the initial snow density ρ_0 at a given site, it is possible to calculate the density at depth, the depth of the $\rho = 0.55$ Mg m^{-3} transition, and the depth–age relationship down to the zone of pore close-off. The value of ρ_0 used is the zero-depth intersection of the line of $\ln [\rho/(\rho_i - \rho)]$ versus depth, which may not be identical with the commonly reported average density over the first one or two meters of snow.

For the initial stage of densification, the density at depth h is:

$$\rho_h = \frac{\rho_i z_0}{1 + z_0}, \tag{7}$$

https://doi.org/10.3189/S0022143000015239 Published online by Cambridge University Press

where $\mathcal{Z}_0 = \exp[\rho_i k_0 h + \ln\{\rho_0/(\rho_i-\rho_0)\}]$. Note the surprising result that the depth–density relationship in this region is independent of the accumulation rate. The depth at which the "critical density" is reached is, by rearrangement,

$$h_{0.55} = \frac{1}{\rho_i k_0}\left[\ln\left(\frac{0.55}{\rho_i-0.55}\right) - \ln\left(\frac{\rho_0}{\rho_i-\rho_0}\right)\right], \tag{8}$$

and the age in years at this depth is

$$t_{0.55} = \frac{1}{k_0 A}\ln\left[\frac{\rho_i-\rho_0}{\rho_i-0.55}\right]. \tag{9}$$

Intermediate depths and ages may be calculated by substituting appropriate values of ρ into Equations (8) and (9).

For the second stage of densification, the density at depth h is

$$\rho_h = \frac{\rho_i \mathcal{Z}_1}{1+\mathcal{Z}_1}, \tag{10}$$

where $\mathcal{Z}_1 = \exp[\rho_i k_1 (h-h_{0.55})/A^{0.5} + \ln\{0.55/(\rho_i-0.55)\}]$. The age of firn at density ρ is

$$t_\rho = \frac{1}{k_1 A^{0.5}}\ln\left(\frac{\rho_i-0.55}{\rho_i-\rho}\right) + t_{0.55}. \tag{11}$$

The mean annual accumulation rate may be estimated from the slope C' of the second stage of densification and the mean annual temperature:

$$A = \left(\frac{\rho_i k_1}{C'}\right)^2. \tag{12}$$

The effects of independently varying the temperature and accumulation rate on the profile of $\ln[\rho/(\rho_i-\rho)]$ predicted by this model are shown in Figure 2. In Figure 2a, the accumulation rate is held constant at 0.3 m water year^{-1} and the initial density is 0.36 Mg m^{-3}. For temperatures from -15°C to -40°C, the depth at which the "critical density" of 0.55

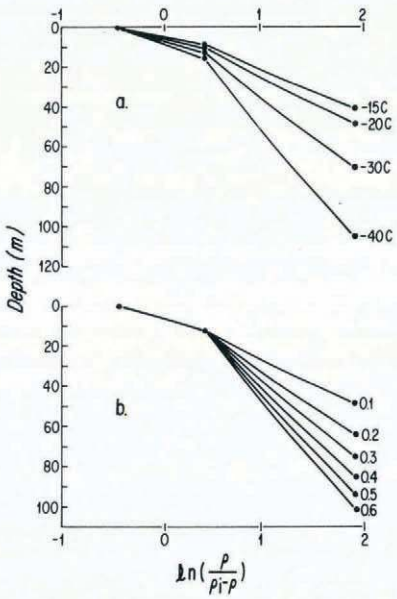

Fig. 2. Predicted depth–$\ln[\rho/(\rho_i-\rho)]$ *curves for: (a) various temperatures at a constant accumulation rate of 0.30 m water year*$^{-1}$ *and initial density of 0.36 Mg m*$^{-3}$*, and (b) various accumulation rates (in m water year*$^{-1}$*) at a constant temperature of* -30°*C and initial density 0.36 Mg m*$^{-3}$.

https://doi.org/10.3189/S0022143000015239 Published online by Cambridge University Press

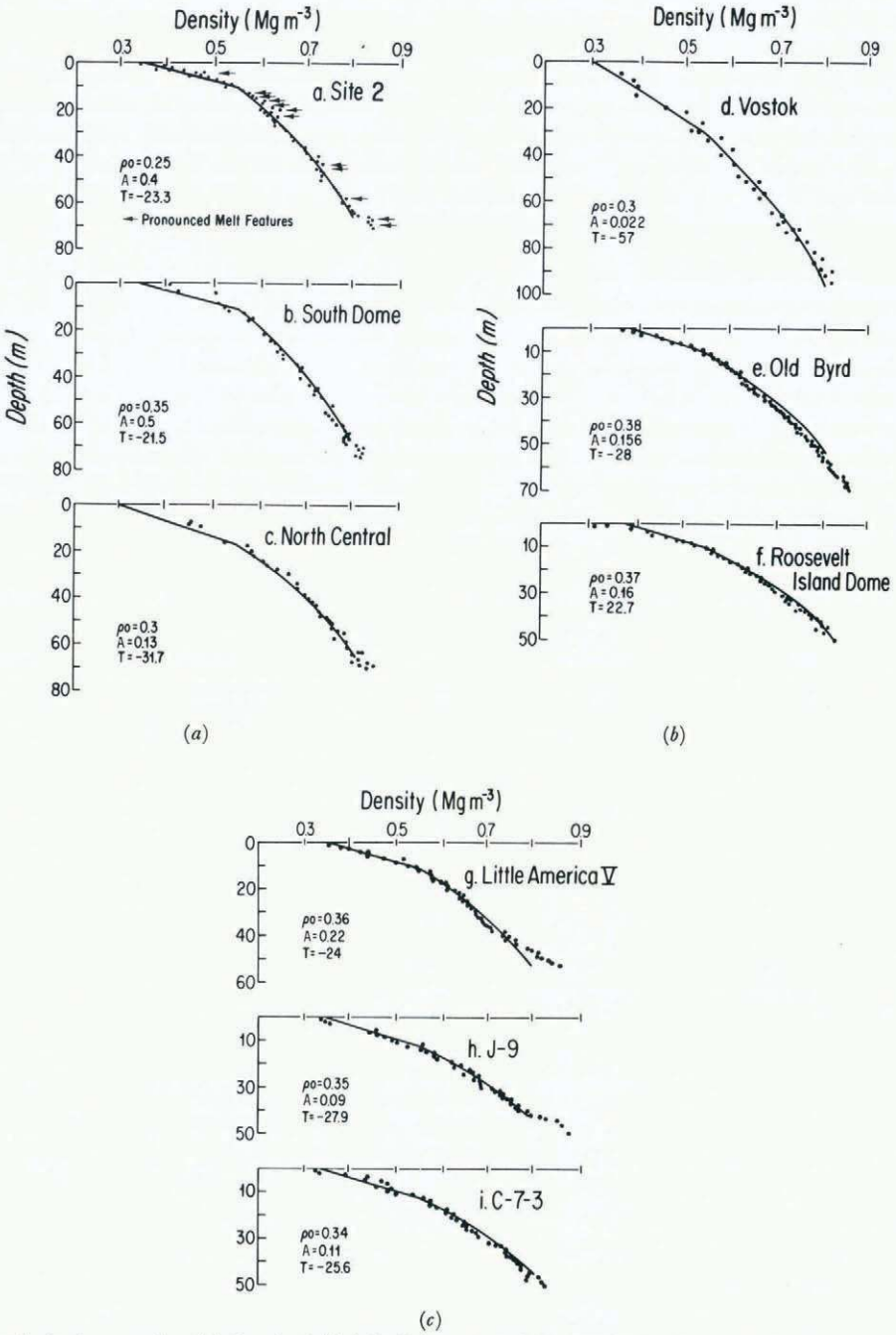

Fig. 3. Depth–density curves for: (a) Greenland, (b) inland Antarctic, and (c) Ross Ice Shelf ice cores. Initial density, accumulation rate, and temperature values shown were used to generate model curves shown as solid lines. Arrows in the Site 2 profile refer to pronounced melt features (Langway, 1970).

https://doi.org/10.3189/S0022143000015239 Published online by Cambridge University Press

Mg m^{-3} is reached varies from 9.3 m to 15.5 m. At −15°C the density attains a value of 0.8 Mg m^{-3} at a depth of 44 m and an age of 93 years. The corresponding values at −40°C are 115 m and 254 years.

In Figure 2b the temperature is held constant at −30°C, the initial density is again 0.36 Mg m^{-3}, and the accumulation rate is varied from 0.1 to 0.6 m water year^{-1}. As noted previously, the first-stage depth–density curve is independent of the accumulation rate. The density reaches a value of 0.8 Mg m^{-3} at 49 m for $A = 0.1$ compared to a depth of 102 m for $A = 0.6$ m water year^{-1}. However, this process requires only 113 years for $A = 0.6$ compared to 310 years for $A = 0.1$ m water year^{-1}.

Comparison with observation

Depth–density data from inland Greenland (Site 2, South Dome, North Central), inland Antarctica (Vostok, Old Byrd, Roosevelt Island Dome) and the Ross Ice Shelf, Antarctica (Little America V, J-9, C-7-3) are shown in Figure 3. Model curves, shown as solid lines, were generated from Equations (7) and (10) using the initial density, temperature, and accumulation rates given. The agreement between observed and predicted profiles for sites with such a wide range of temperatures and accumulation rates demonstrates the usefulness of the model. The density anomalies at 22 m in the Old Byrd profile and at 28 m in the Little America V profile will be discussed more fully in the next section.

Table III. Observed and predicted ages for five ice cores from Greenland and Antarctica

	Crête, Greenland		*Site 2, Greenland*		*Milcent, Greenland*		*Byrd Station, Antarctica*		*Little America V, Antarctica*	
Depth m	*Predicted age*	*Observed*[1] *age*	*Predicted age*	*Observed*[2] *age*	*Predicted age*	*Observed*[3] *age*	*Predicted age*	*Observed*[4] *age*	*Predicted age*	*Observed*[4] *age*
0		1974·5		1957		1973·5		1959		1959
10	1957	1958	1945	*c.* 1945	1964	1964	1929	1927	1938	1937
20	1936	1938	1931	*c.* 1930	1952	1952	1892	1888	1912	1912
30	1912	1914	1915	*c.* 1915	1940	1939	1850	1845	1882	1884
40	1887	1888	1898	*c.* 1900	1926	1925	1804	1802	1853 (39 m)	1854 (39 m)
50	1860	1861	1880	*c.* 1880	1912	1911	1754	1754		
60	1832	1831	1860	*c.* 1860	1896	1894	1703	1703		

[1] Personal communication from W. Dansgaard.
[2] Langway (1970).
[3] Hammer and others (1978); Reeh and others (1978).
[4] Gow (1968).

As a further measure of the scope of this model, Table III compares ages of five ice cores calculated from Equations (9) and (11) with ages determined by stratigraphic techniques (Gow, 1968; Langway, 1970) and by analysis of stable oxygen isotope and microparticle concentration variations (Hammer and others, 1978; Reeh and others, 1978; personal communication from W. Dansgaard). Observed and predicted ages agree to within five years over time spans as great as 256 years, which is very good considering the uncertainties in measurement accuracy, the normal variability in accumulation rates, and the empirical nature of the model.

Table IV compares observed accumulation rates with rates derived using Equation (12). Due to the abundance of ice layers at Dye 2, Maudheim, and Roi Baudouin, these sites were not included in the derivation of the model, and predicted values are included for completeness. The agreement between observed and predicted values is quite good with an average deviation of only 0.04 m water year^{-1} and an average relative deviation of 16%. For dry-

snow and percolation facies, the accumulation rates predicted by this model will generally be within about 20% of the mean over the time period represented in the $\rho < 0.8$ Mg m^{-3} section of core.

TABLE IV. OBSERVED AND PREDICTED ACCUMULATION RATES

Site	*Accumulation rate* m water year^{-1} *Observed*	*Predicted*	*Deviation*	*% deviation*
	Greenland			
North Central	0.13	0.11	−0.02	15
Crête	0.26	0.22	−0.04	15
Milcent	0.50	0.40	−0.10	20
Site 2	0.40	0.39	−0.01	3
South Dome	0.50	0.61	+0.11	22
Dye 3	0.50	0.61	+0.11	22
Dye 2	0.5	0.45	−0.05	10
	Antarctica			
Vostok	0.022	0.019	−0.003	14
South Pole	0.07	0.09	+0.02	29
Old Byrd Station	0.16	0.19	+0.03	19
Roosevelt Island Dome	0.2	0.16	−0.04	20
Wilkes S-2	0.133	0.15	+0.017	13
	Antarctic ice shelves			
J-9	0.09	0.08	−0.01	11
C-7-3	0.11	0.13	+0.02	18
Little America V	0.22	0.22	0.00	0
Maudheim	0.37	0.37	0.00	0
Roi Baudouin	0.38	0.54	+0.16	42

DENSITY PROFILES AS CLIMATIC INDICATORS

Discrepancies between observed and predicted density profiles should be indicative of climatic conditions, since the pertinent variables are temperature, accumulation rate, and the presence of ice layers. This concept is best demonstrated with the ice cores from Site 2, Old Byrd Station, and Little America V, where long-term accumulation-rate records are available, the density values have been averaged over essentially every meter of depth, and the cores were obtained by mechanical, rather than thermal, drilling techniques (Gow, 1968; Langway, 1970).

The most pronounced melt features in the 0–70 m depth interval of the Site 2 core (Langway, 1970) are indicated by arrows in Figure 3a. The observed and predicted densities are in excellent agreement throughout most of the core, and a clear correspondence may be seen between the presence of ice layers and abnormally high densities. Without the predicted profile for comparison, such features might have been ascribed to scatter in the data.

Anomalous intervals of constant density may be clearly seen at a depth of 22 m in the Old Byrd Station core and at the 28 m depth in the Little America V core. Above these depths, observed and predicted densities are in excellent agreement. Below these depths the profiles are parallel but separated by a 2 or 3 m interval. The very high densification rate at Little America V, which begins at 35 m and continues through the pore close-off depth, has been attributed to local areas of high stress (Gow, 1968). Similar sudden departures between observed and predicted profiles may be seen, although not so clearly, at about the 25 m depth in the Roosevelt Island Dome core and at a depth of 20 m in the C-7-3 core: The depths of these intervals of constant density are in general agreement with the depths of anomalies in the velocity-gradient profiles of compressional wave, "C" depths, reported to occur over widespread areas of West Antarctica (Robertson and Bentley, 1975). It was

suggested that seismic anomalies, identifiable only in areas of relatively high accumulation rates, represent a transition to an intermediate stage of densification where a different mechanism of metamorphism predominates (Robertson and Bentley, 1975). However, the slopes of the depth—ln $[\rho/(\rho_i-\rho)]$ lines are identical above and below the depths of the anomalies (see Appendix) implying a uniform densification mechanism. There are no intervals of constant density or other anomalies in the profiles of Greenland sites such as Site 2 and South Dome as would be expected if the identification of an additional densification stage were facilitated by greater accumulation rates.

According to the model, an interval of negligible densification might be produced by a long time period of much lower temperature or by a short time period of high accumulation. A high-accumulation event would seem the more likely to occur in Nature. This concept is supported by the fact that within the uncertainties of the dating techniques the depths of the density anomalies may be regarded as synchronous. Stratigraphically determined dates are A.D. 1880 at Old Byrd Station and A.D. 1890 at Little America V (Gow, 1968). Model age calculated from Equations (9) and (11) are A.D. 1883 and A.D. 1885 respectively. Model depths for the A.D. 1885 horizon at other West Antarctic and Ross Ice Shelf locations are 26 m at Roosevelt Island Dome, 20 m at C-7-3, and 17 m at J-9, in good agreement with depths of the density anomalies. Model ages of the seismic "C" depth anomaly, calculated from the data of Robertson and Bentley (1975) for the Little America V–Byrd and Sentinel traverses give a mean date of A.D. 1882 ± 34 years. The high degree of scatter is probably due to the combined uncertainties in the accumulation rate and in the "C" depths.

The depth intervals of constant density and deviations between observed and predicted profiles indicate that accumulation rates were greater by a factor of about ten rather than a constant amount at each station. From the accumulation rates and densities at the anomalous zone, ten times the mean annual accumulation would represent the following depth intervals: 3 m at Little America V, 2.3 m at Old Byrd Station, 2.2 m at Roosevelt Island Dome, 1.7 m at C-7-3, and 1.4 m at J-9. These values are in good agreement with the observed intervals, and the concept explains the failure to observe density anomalies or seismic "C" depths at stations with low accumulation rates. Although the intervals of constant density may in fact be merely due to measurement errors, it will be interesting to see if the effects of the Krakatau (1883) eruption are found at the same depths. Known episodes of explosive volcanic activity, including the Krakatau eruption, have been detected by chemical analysis of the Milcent ice core (Herron and Langway, 1978).

Summary

Empirical rate equations describing the first and second stages of densification have been derived from Greenland and Antarctic ice-core densities. Using these rate equations it is possible to predict depth–density curves and depth–age relationships in polar ice sheets and ice shelves. The only parameters required are the mean annual temperature, annual accumulation rate, and the initial snow density. These can often be determined in the course of a single 10 m deep core drilling operation. Given the mean annual temperature and second stage depth–density data, it is possible to predict the annual accumulation rate to within about 20% of values obtained by other techniques.

Deviations between observed and predicted depth–density profiles may be related to changing climatic conditions. Abnormally high densities at Site 2 are coincident with prominent melt features indicative of unusual summer warmth. Depth intervals of constant density at Old Byrd, Little America V, and possibly at C-7-3, J-9–Roosevelt Island Dome may reflect a synchronous "event" occurring in the 1880's when large portions of the Antarctic continent received as much as ten times the normal snowfall within a year or two.

ACKNOWLEDGEMENTS

This study was only made possible by the field efforts of many individuals: including ice-core drilling engineers (B. L. Hansen, J. Rand, H. Rufli, S. Johnsen, and J. Nielsen) and glaciologists (J. Cragin, E. Chiang, K. Miller, and S. Herron). Most of the Greenland field work was performed under the aegis of the combined U.S.–Danish–Swiss Greenland Ice Sheet Program. This paper was kindly reviewed by G. de Q. Robin and C. Benson. Both field and laboratory research was sponsored by the Division of Polar Programs, National Science Foundation.

MS. received 12 December 1978 and in revised form 2 July 1979

APPENDIX

DEPTH–ln $[\rho/(\rho_1-\rho)]$ PROFILE

THIS Appendix contains depth–ln $[\rho/(\rho_1-\rho)]$ data for ice cores from inland Greenland (Fig. A1), inland Antarctica (Fig. A2), and the Ross Ice Shelf, Antarctica (Fig. A3). For aid in interpretation of the profiles, Table V gives conversions of density to values of ln $[\rho/(\rho_1-\rho)]$.

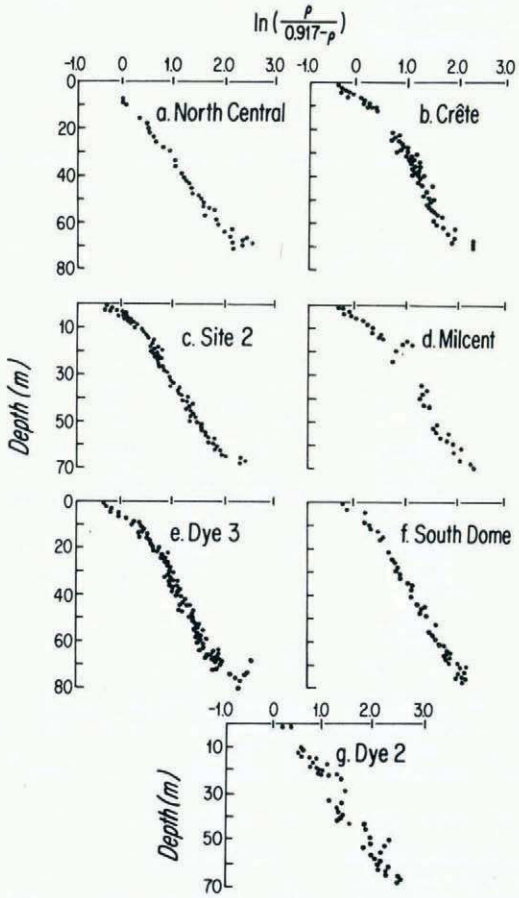

*Fig. A1. Depth–*ln $[\rho/(\rho_1-\rho)]$ *data for inland Greenland sites.*

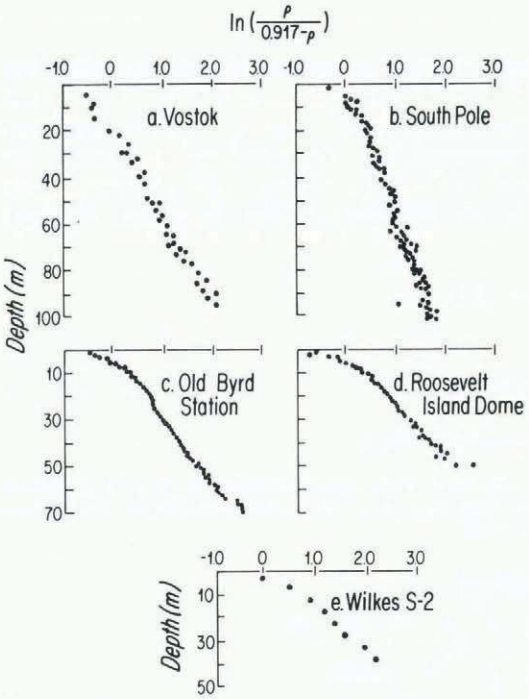

*Fig. A2. Depth–*ln $[\rho/(\rho_1-\rho)]$ *data for inland Antarctic sites.*

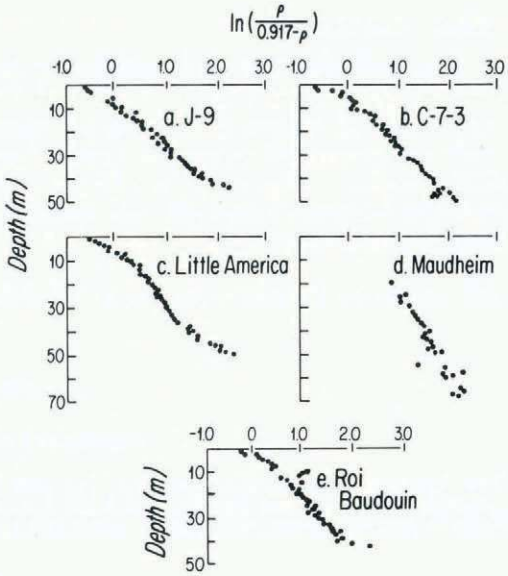

*Fig. A3. Depth–*ln $[\rho/(\rho_1-\rho)]$ *data for Ross Ice Shelf, Antarctica sites.*

TABLE V. DENSITY–ln $[\rho/(\rho_1-\rho)]$ VALUES

Density Mg m^{-3}	ln $[\rho/(\rho_1-\rho)]$
0.35	−0.48
0.40	−0.26
0.45	−0.04
0.50	0.18
0.55	0.40
0.60	0.64
0.65	0.89
0.70	1.17
0.75	1.50
0.80	1.92
0.82	2.13
0.84	2.39

REFERENCES

Anderson, D. L., *and* Benson, C. S. 1963. The densification and diagenesis of snow. (*In* Kingery, W. D., *ed. Ice and snow; properties, processes, and applications: proceedings of a conference held at the Massachusetts Institute of Technology, February 12–16, 1962.* Cambridge, Mass., The M.I.T. Press, p. 391–411.)

Bader, H. 1954. Sorge's law of densification of snow on high polar glaciers. *Journal of Glaciology*, Vol. 2, No. 15, p. 319–23.

Bader, H. 1960. Theory of densification of dry snow on high polar glaciers. *U.S. Snow, Ice and Permafrost Research Establishment. Research Report* 69.

Bader, H. 1962. Theory of densification of dry snow on high polar glaciers, 2. *U.S. Cold Regions Research and Engineering Establishment. Research Report* 108.

Bader, H. 1965. Theory of densification of dry, bubbly glacier ice. *U.S. Cold Regions Research and Engineering Laboratory. Research Report* 141.

Barkov, N. I. 1973. Rezul'taty issledovaniya skvazhiny i ledyanogo kerna na stantsii Vostok v 1970–1972 gg. [Results of the study of the bore hole and ice core at Vostok Station in 1970–72]. *Materialy Glyatsiologicheskikh Issledovaniy. Khronika. Obsuzhdeniya*, Vyp. 22, p. 77–81.

Barkov, N. I., *and others*. 1974. Pervyye resul'taty izucheniya ledyanogo kerna iz skvazhiny so stantsii Vostok (Antarktida) isotopno-kislorodnym metodom [First results of studying an ice core from Vostok Station bore hole (Antarctica) by an oxygen isotope method]. [By] N. I. Barkov, F. G. Gordiyenko, Ye. S. Korotkevich, V. M. Kotlyakov. *Doklady Akademii Nauk SSSR*, Tom 214, No. 6, p. 1383–86.

Benson, C. S. 1959. Physical investigations on the snow and firn of northwest Greenland 1952, 1953, and 1954. *U.S. Snow, Ice and Permafrost Research Establishment. Research Report* 26.

Benson, C. S. 1962. Stratigraphic studies in the snow and firn of the Greenland ice sheet. *U.S. Snow, Ice and Permafrost Research Establishment. Research Report* 70.

Butkovich, T. R. 1953. Density of single crystals of ice from a temperate glacier. *U.S. Snow, Ice and Permafrost Research Establishment. Research Paper* 7.

Clausen, H. B., *and* Dansgaard, W. 1977. Less surface accumulation on the Ross Ice Shelf than hitherto assumed. [*Union Géodésique et Géophysique Internationale. Association Internationale des Sciences Hydrologiques. Commission des Neiges et Glaces.*] *Symposium. Isotopes et impuretés dans les neiges et glaces. Actes du colloque de Grenoble, août/septembre 1975*, p. 172–76. (IAHS–AISH Publication No. 118.)

Costes, N. C. 1963. On the process of normal snow densification in an ice cap. (*In* Kingery, W. D., *ed. Ice and snow; properties, processes, and applications: proceedings of a conference held at the Massachusetts Institute of Technology, February 12–16, 1962*. Cambridge, Mass., The M.I.T. Press, p. 412–31.)

Gow, A. J. 1968. Deep core studies of the accumulation and densification of snow at Byrd Station and Little America V, Antarctica. *U.S. Cold Regions Research and Engineering Laboratory. Research Report* 197.

Gow, A. J. [1975.] Time–temperature dependence of sintering in perennial isothermal snowpacks. [*Union Géodésique et Géophysique Internationale. Association Internationale des Sciences Hydrologiques. Commission des Neiges et Glaces.*] *Symposium. Mécanique de la neige. Actes du colloque de Grindelwald, avril 1974*, p. 25–41. (IAHS–AISH Publication No. 114.)

Hammer, C. U., *and others*. 1978. Dating of Greenland ice cores by flow models, isotopes, volcanic debris, and continental dust, by C. U. Hammer, H. B. Clausen, W. Dansgaard, N. Gundestrup, S. J. Johnsen, and N. Reeh. *Journal of Glaciology*, Vol. 20, No. 82, p. 3–26.

Herron, M. M., *and* Langway, C. C., *jr*. 1978. Impact of volcanic eruptions on atmospheric composition as revealed in Greenland ice sheet strata. *Geological Society of America. Abstracts with Programs*, Vol. 10, No. 7, p. 420.

Hobbs, P. V. 1968. Metamorphism of dry snow at a uniform temperature. *Union de Géodésie et Géophysique Internationale. Association Internationale d'Hydrologie Scientifique. Assemblée générale de Berne, 25 sept.–7 oct. 1967.* [*Commission de Neiges et Glaces.*] *Rapports et discussions*, p. 392–402. (Publication No. 79 de l'Association Internationale d'Hydrologie Scientifique.)

Hollin, J. T., *and* Cameron, R. L. 1961. I.G.Y. glaciological work at Wilkes Station, Antarctica. *Journal of Glaciology*, Vol. 3, No. 29, p. 833–43.

Johnsen, S. J. 1977. Stable isotope homogenization of polar firn and ice. [*Union Géodésique et Géophysique Internationale. Association Internationale des Sciences Hydrologiques. Commission des Neiges et Glaces.*] *Symposium. Isotopes et impuretés dans les neiges et glaces. Actes du colloque de Grenoble, août/septembre 1975*, p. 210–19. (IAHS–AISH Publication No. 118.)

Kohnen, H. 1972. Über die Beziehung zwischen seismischen Geschwindigkeiten und der Dichte in Firn und Eis. *Zeitschrift für Geophysik*, Bd. 38, Ht. 5, p. 925–35.

Kojima, K. 1964. Densification of snow in Antarctica. (*In* Mellor, M., *ed. Antarctic snow and ice studies*. Washington, D.C., American Geophysical Union, p. 157–218. (Antarctic Research Series, Vol. 2.))

Langway, C. C., *jr*. 1958. Bubble pressures in Greenland glacier ice. *Union Géodésique et Géophysique Internationale. Association Internationale d'Hydrologie Scientifique. Symposium de Chamonix, 16–24 sept. 1958*, p. 336–49. (Publication No. 47 de l'Association Internationale d'Hydrologie Scientifique.)

Langway, C. C., *jr*. 1970. Stratigraphic analysis of a deep ice core from Greenland. *Geological Society of America. Special Paper* 125.

Nye, J. F. 1963. Correction factor for accumulation measured by the thickness of the annual layers in an ice sheet. *Journal of Glaciology*, Vol. 4, No. 36, p. 785–88.

Reeh, N., *and others*. 1978. Secular trends of accumulation rates at three Greenland stations, by N. Reeh, H. B. Clausen, W. Dansgaard, N. Gundestrup, C. U. Hammer, and S. J. Johnsen. *Journal of Glaciology*, Vol. 20, No. 82, p. 27–30.

Robertson, J. D., *and* Bentley, C. R. 1975. Investigation of polar snow using seismic velocity gradients. *Journal of Glaciology*, Vol. 14, No. 70, p. 39–48.

Robin, G. de Q. 1958. Glaciology. III. Seismic shooting and related investigations. *Norwegian–British–Swedish Antarctic Expedition, 1949–52. Scientific Results*, Vol. 5.

Schytt, V. 1958. Glaciology. II. Snow studies at Maudheim.—Snow studies inland.—The inner structure of the ice shelf at Maudheim as shown by core drilling. *Norwegian–British–Swedish Antarctic Expedition, 1949–52. Scientific Results*, Vol. 4, A, B, C.

Tongiorgi, E., *and others*. 1962. Deep drilling at Base Roi Baudouin, Dronning Maud Land, Antarctica, by E. Tongiorgi, E. [E.] Picciotto, W. de Breuck, T. Norling, J. Giot, and F. Pantanetti. *Journal of Glaciology*, Vol. 4, No. 31, p. 101–10.